Key Engineering Materials Vol. 497 (2012) pp 285-295

doi:10.4028/www.scientific.net/KEM.497.285

Single Inductor DC-DC Converter with Independent Bipolar Outputs using Charge Pump

Nobukazu Takai[1a], Kenji Takahashi[1], Hajime Yokoo[1], Shunsuke Miwa[1], Kengo Tsushida[1],
Hiroyuki Iwase[1], Kazuki Murakami[1], Haruo Kobayashi[1], Takahiro Odaguchi[2], Shigeki Takayama[2], Takeshi Oomori[2], Isao Nakanishi[2], Kenji Nemoto[2] and Jun-ichi Matsuda[3]

[1]Graduate School of Electrical Engineering, Faculty of Engineering
Gunma University, Gunma, Japan 378–8515

[2]AKM Technology Corporation

[3]Asahi Kasei Power Devices Corporation
[a]takai@gunma-u.ac.jp(corresponding author)

Keywords: Single-Inductor Bipolar Output, DC-DC Converter, Pseudo-continuous conduction mode (PCCM), Charge Pump

Abstract. This paper describes a bipolar output DC-DC converter that uses a single inductor for size and cost reduction. We propose a timing diagram for a charge pump circuit which generates the negative output voltage, and present its configuration, operation principle and simulation results. We also show that employing pseudo-continuous conduction mode improves cross-regulation between the two outputs.

Introduction

Portable devices such as cellular phones, PDA's, game appliances, and so on, have become a large and lucrative market for switching power IC's. Switching regulators are suitable for the power supply circuit of the mobile equipment because of its high efficiency, small size, and low power consumption characteristics. Low cost, high efficiency and extremely small system solutions are critical to success, but the demands are quite conflicting.

The active matrix Organic Electro Luminescence (AMOEL) display is a strong candidate for mobile applications owing to its high resolution, low power consumption and low cost. AMOEL panels, however, usually require bipolar power supplies with different regulated voltages. Therefore, boost switching converters that can supply bipolar outputs for this application are important.

Single-inductor multiple-output (SIMO) switching converters can support more than one output while requiring only one off-chip inductor, which yields many appealing advantages for mass-production and applications. The SIMO boost switching converter is reported in [1–7]. The SIMO converter works in pseudo-continuous conduction mode (PCCM) with a freewheel period, which help to handle large load currents and eliminate cross-regulation [8–10]. PCCM technique is suitable for SIMO converter because of its advantage for cross-regulation.

In [1], SIMO switching converter with bipolar outputs using charge pump, is proposed. However the negative output voltage of [1] depends on its positive output voltage. This feature restricts the possible applications for that particular converter.

In this paper, a single inductor bipolar outputs (SIBO) DC-DC converter is proposed. In order to realize independence of each output voltage, we propose a new timing diagram for use with the conventional circuitry. The bipolar outputs of the converter can vary its output voltage by duty ratio independently. Simulations are performed to verify the proposed method. Simulation results of transient analysis with the Spectre simulator indicate that the positive output voltage remains constant even with variations in the negative output voltage using the proposed timing diagram, while the negative output voltage depends on the positive output voltage using the conventional timing diagram. Simulation results also indicate that the proposed method maintains goal cross-regulation of both outputs.

SIBO DC-DC Converter

Continuous-Conduction-Mode, Discontinuous-Conduction-Mode, and Pseudo-Continuous-Conduction-Mode. A DC-DC Converter has three operation modes for the current control in the energy transfer inductor : Continuous-Conduction-Mode (CCM), Discontinuous-Conduction-Mode (DCM), and Pseudo-Continuous-Conduction-Mode(PCCM). In Fig.1(a), CCM means that the current

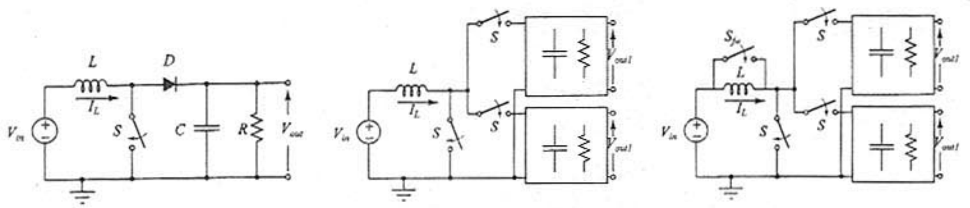

(a) Basic boost converter circuit. (b) SIBO circuit. (c) SIBO circuit with Freewheel switch.

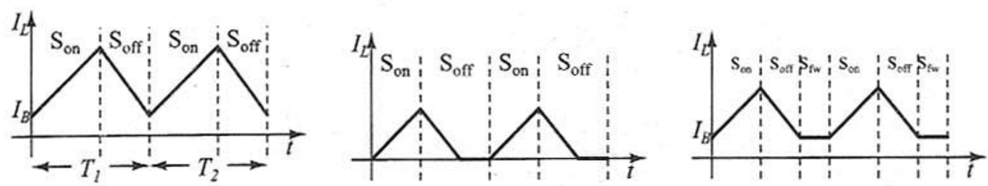

(d) Waveform of inductor current using CCM. (e) Waveform of inductor current using DCM. (f) Waveform of inductor current using PCCM.

Fig. 1: Wave form of inductor current using CCM, DCM, and PCCM.

I_L in the energy transfer inductor L never goes to zero between switching cycles as shown in Fig.1(d), while in DCM, the current goes to zero during part of the switching cycle as shown in Fig.1(e). The advantage of CCM is that the ripple of the inductor current of CCM is smaller than that of DCM when same energy is applied to a load. The advantage of DCM is that the transfer function is first-order so system is stable while that of CCM is second-order. When we try to realize Single Inductor Bipolar Output DC-DC Converter as shown in Fig.1(b), the inductor current is shared for each output terminal. Because two outputs share one inductor in turns, we must take the effect of current variation of each output terminal into account. When CCM is employed for the control of the inductor current, the current variation of one output terminal affects the current of other terminal because inductor current is continuous when switch S_{off} turns to S_{on} as shown in Fig.1(d). This effect is called cross-regulation, and cross-regulation is not good if CCM is employed for control of the inductor current. DCM has good cross-regulation characteristics because the inductor current is not contiguous when switch S_{off} turns to S_{on}. However the inductor current ripple is not small. In order to solve this problem, PCCM is proposed in [10]. Figure 1(f) indicates the waveform of inductor current using PCCM. In PCCM, the floor of the inductor current is raised by a DC level of I_B. PCCM can realize small inductor current ripple as in DCM case. Compared with the CCM case, the inductor current alternately resets and stays constant at I_B which successfully isolates the two output current variations. Individual output current variation can be adjusted by changing the duty ratio of S_{on} and S_{off} of corresponding output terminal, which does not affect the other. To achieve PCCM, we must realize a constant inductor current. Switch S_{fw} in Fig.1(c) keeps the inductor current constant which is called the freewheelin switch.

Circuit schema and conventional timing diagram. Figure 2(a) indicates single-inductor multiple-output switching converter [1]. The switching converter of Fig. 2(a) consists of a boost converter, a charge pump, and a freewheel switch. The converter can supply bipolar outputs by using conventional timing diagram of Fig. 2(a). The conventional timing diagram is composed of three regions i.e. ``stage 1," ``stage 2," and ``stage 3" as shown in Fig.2(b). In order to find bipolar outputs of the converter, circuit equations of each region are given as follows.

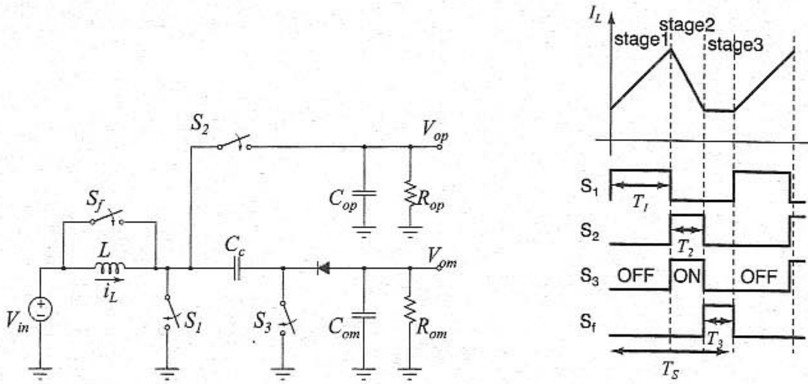

(a) SIMO DC-DC converter schematic [1].

(b) Conventional timing diagram.

Fig. 2: Single inductor bipolar outputs DC-DC converter with charge pump.

region "stage 1"

Only switch S_1 turns on, so inductor L stores energy from the voltage source V_{in}. Relations between the inductor current i_L, the input voltage V_{in}, and the positive output voltage V_{op} are found as

$$\frac{d}{dt}i_L = \frac{V_{in}}{L}, \tag{1}$$

$$\frac{d}{dt}V_{op} = -\frac{V_{op}}{R_{op}C_{op}}. \tag{2}$$

region "stage 2"

Only switch S_2 turns on, so the inductor L supplies its energy to output terminal of V_{op} and charges C_{op}. Thus relations between i_L, V_{in}, and V_{op} become

$$\frac{d}{dt}i_L = \frac{V_{in}-V_{op}}{L}, \tag{3}$$

$$\frac{d}{dt}V_{op} = \frac{i_L}{C_{op}} - \frac{V_{op}}{R_{op}C_{op}}. \tag{4}$$

In this phase, because both switch S_2 and S_3 turn on, the voltage of C_c becomes V_{op}.

region "stage 3"

Freewheel switch S_f turns on and the inductor L keeps its energy and realize PCCM.

region "stage 1(next phase)"

Because switch S_1 turns on and the voltage of C_c is V_{op}, the negative output voltage V_{om} is given by:

$$V_{om} = -V_{op} + V_F, \tag{5}$$

where V_F is the diode voltage drop. Eq.(5) shows that the negative output voltage depends on the positive output voltage.

From Eq.(1)--Eq.(4), we can get state-space averaging equation as

$$\frac{d}{dt}\begin{pmatrix} i_L \\ V_{op} \end{pmatrix} = \begin{pmatrix} 0 & -\frac{D_2}{L} \\ \frac{D_2}{C_{op}} & -\frac{D_1+D_2}{R_{op}C_{op}} \end{pmatrix}\begin{pmatrix} i_L \\ V_{op} \end{pmatrix} + \begin{pmatrix} \frac{D_1+D_2}{L} \\ 0 \end{pmatrix} V_{in}, \tag{6}$$

where D_1 and D_2 are duty ratio of ``stage 1" and ``stage 2" i.e. T_1/T_s and T_2/T_s, respectively. From the stage-space averaging equation, the positive output voltage V_{op} is found as

$$V_{op} = \frac{D_1 + D_2}{D_2} V_{in}. \tag{7}$$

Eq.(7) indicates that the conventional timing diagram can control V_{op} with the duty ratio D_1 and D_2, however Eq.(5) shows V_{om} is dependent of V_{op}. These results restrict the application field of Fig.2(a).

In next section, we propose new timing diagram which the negative output voltage is independent of the positive output voltage.

Proposed timing diagram Figure 3 shows the proposed timing diagram. The proposed timing

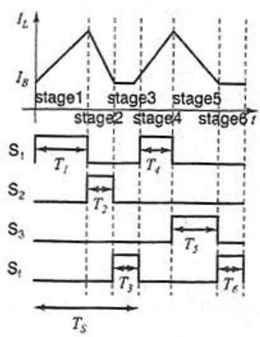

Fig. 3: Proposed timing diagram.

diagram has 6 stages and is applied to the same circuit of Fig.2(a). The timing diagram is separated into two phases, i.e. one phase for the positive voltage, the other for the negative voltage. The ``stage 1" and ``stage 2" determine the positive output voltage, and the ``stage 4" and ``stage 5" the negative output voltage, respectively. Circuit equations of each region are given as follows.

"stage 1"~ "stage 3"

In these stages, analysis is performed in the same way as subsection , and the same equations are obtained. Thus state-space averaging equation for V_{op} becomes the same and V_{op} is obtained as Eq.(7).

"stage 4"

Because only switch S_1 turns on, inductor L stores energy from voltage source V_{in} again. Relations between inductor current i_L, the input voltage V_{in}, and negative output voltage V_{om} are given as

$$\frac{d}{dt}i_L = \frac{V_{in}}{L}, \tag{8}$$

$$\frac{d}{dt}V_{om} = \frac{i_L}{C_{om}} - \frac{V_{om}}{R_{om}C_{om}}. \tag{9}$$

"stage 5"

Since switch S_3 turns on, charge pump capacitor C_c charges energy from the inductor L. Thus relations between i_L, V_{in}, and V_{om} becomes

$$\frac{d}{dt}i_L = \frac{V_{in} - V_{om}}{L}, \tag{10}$$

$$\frac{d}{dt}V_{om} = -\frac{V_{om}}{R_{om}C_{om}}. \tag{11}$$

"stage 6"

Freewheel switch S_f turns on and the inductor L keeps its energy. From Eq.(8)--Eq.(11), state-space averaging equation is found as

$$\frac{d}{dt}\begin{pmatrix} i_L \\ V_{om} \end{pmatrix} = \begin{pmatrix} 0 & -\frac{D_5}{L} \\ \frac{D_4}{C_{om}} & -\frac{D_4+D_5}{R_{om}C_{om}} \end{pmatrix}\begin{pmatrix} i_L \\ V_{om} \end{pmatrix} + \begin{pmatrix} \frac{D_4+D_5}{L} \\ 0 \end{pmatrix} V_{in}, \tag{12}$$

where D_4 and D_5 are duty ratios of ``stage 4" and ``stage 5" i.e. T_4/T_s and T_5/T_s, respectively. From Eq.(12), the negative output voltage V_{om} is found as

$$V_{om} = -\frac{D_4 + D_5}{D_5}V_{in} + V_F. \tag{13}$$

Eq.(13) indicates that V_{om} can be controlled with the duty ratio D_4 and D_5 and is independent of V_{op}.

Control Circuitry

In order to obtain the proposed timing diagram, a control circuit which consists of three components is required. One component is to divide the period with respect to positive and negative output voltage. The second component is to detect the inductor current i_L and limit the inductor current to I_B. The final component is a logic circuit to avoid not overlapping the timing of all switches. Figure 4 indicates whole proposed circuit with the control circuit blocks. The control circuit blocks are composed of resistors for dividing the output voltages, EAs(Error Amplifiers), reference voltage source, two ramp wave generators, CMPs(Comparators), Logic Circuit, and current sensor.

Current sensor In order to limit the lowest inductor current to I_B, a current sensor for the inductance current is required. Figure 5 shows the detection circuit of the inductance current. Resistor r_L is connected to the inductance in series as shown in Fig.4. The output voltage V_{cs} controls the freewheel switch S_f. The inductor current i_L is detected as voltage $V_r = r_L i_L$. The reference voltage V_{ibref} is set to $V_{ibref} = r_L I_B$ and is compared with V_r. When the inductor current i_L becomes I_B, the output voltage V_{cs} turns on. V_{cs} is applied to the logic circuit and is utilized for the control signal of the freewheel switch.

Sawtooth wave generator For the division of the period of positive voltage and negative voltage, exclusive sawtooth wave shown in Fig.6 is required. Figure 7 indicates employed circuit which

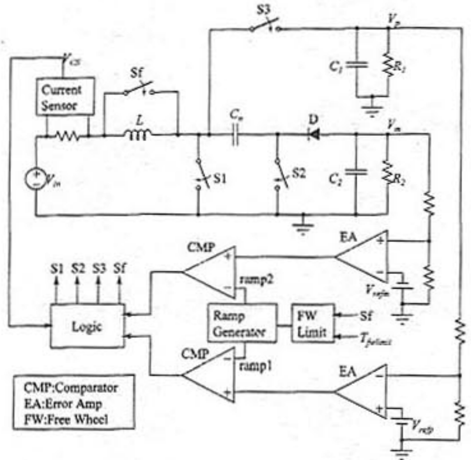

Fig. 4: Proposed DC-DC converter with control circuit

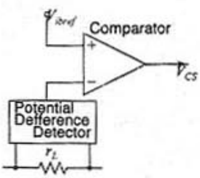

Fig. 5: Current Sensor

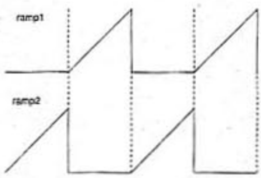

Fig. 6: Employed exclusive sawtooth wave

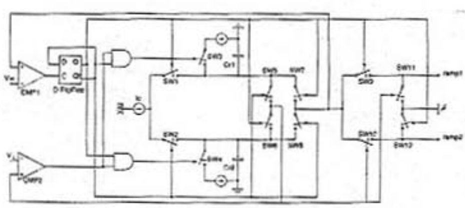

Fig. 7: Proposed sawtooth wave generation circuit

generate the sawtooth wave as shown in Fig.6 [11]. Detail operation is omitted which is described in [11]. Using this circuit, we can obtain exclusive output voltage ramp1 and ramp2 as shown in Fig.6 by using Fig.7.

Logic circuit The logic circuit shown in Fig.8 is used to avoid overlapping the timing of all switches. We explain the operation of this logic circuit. As an initial condition, the outputs of both

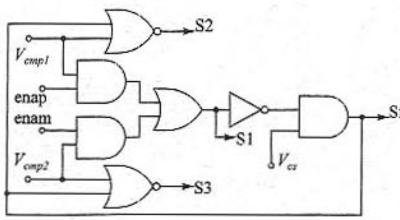

Fig. 8: logic circuit

comparators are high. A pulse signal is applied to ``enap" to select the positive output terminal and to ``enam" to select negative output terminal. V_{CS} is the output voltage of the current sensor.

T1: Because V_{comp1} and enap are high, S1 goes high.

T2: V_{comp1} goes low, and S2 turns on.

T3: Inductor current reaches I_B, and V_{CS} goes high, hence Sf goes high.

T4: Pulse signal is applied to ``enap," so S1 goes high.

T5: Because V_{comp2} goes low, S3 turns on.

T6: Because the inductor current reaches I_B, and V_{CS} goes high, Sf goes high.

Simulation results

Simulations are performed to verify the proposed timing diagram using the Spectre circuit simulator. Figure 4 is used for verification. Parameters used in the simulations are shown in Table 1.

Table 1: Simulation conditions

Input voltage V_{in}	3.5V
switching frequency	500kHz
inductor	2μH
output capacitance C_{op}, C_{om}	10μF
load resistance	15Ω
charge pump capacitance C_c	5μF
on resistance	10mΩ
diode drop voltage	0.85V

Figure 9 indicates the simulation result for the sawtooth wave generator. We can see from Fig.9 that the circuit of Fig.7 can apply independent sawtooth outputs.

Figures 10 and 11 show transient responses of the converter.

Figures 10(a) and 10(b) show simulation results of transient response using the conventional timing diagram of Fig.2(b). In order to confirm that V_{om} depends on V_{op} as given by Eq.(5), simulations are performed under two conditions. V_{op} and V_{om} using the conventional timing diagram, are obtained from Eqs.(5) and (7). Duty ratio is set to $D_1 = D_2 = 0.4$, i.e. $V_{op} = 7.0$V and $V_{om} =$

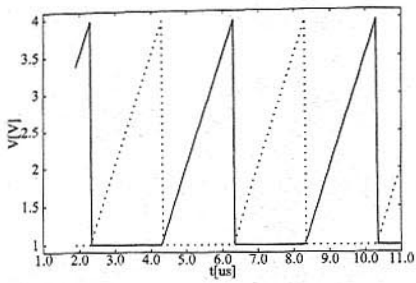

Fig. 9: Simulation result of the Sawtooth Wave Generator

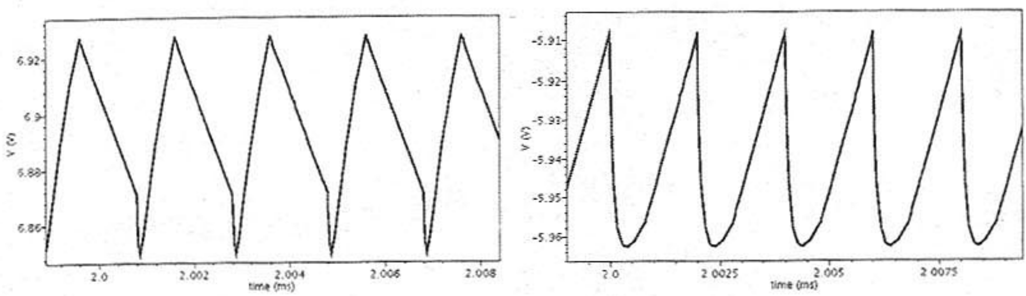

Positive output voltage. Negative output voltage.

(a) Simulation results under condition 1.

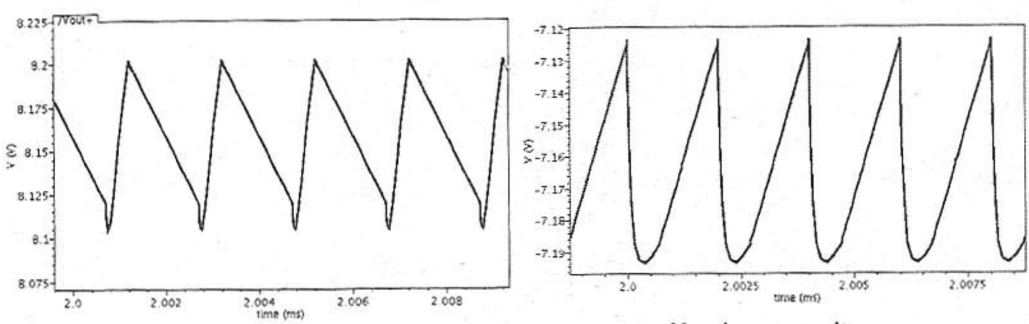

Positive output voltage. Negative output voltage.

(b) Simulation results under condition 2.

Fig. 10: Transient responses using the conventional timing diagram.

-6.15V(Condition 1), and $D_1 = 0.35$, $D_2 = 0.25$, i.e. $V_{op} = 8.4$V and $V_{om} = -7.55$V(Condition 2). We can see from Figs. 10(a) and 10(b) that V_{op} reaches the theoretical value and V_{om} varies by V_{op} of Eq.(5).

Figures 11 indicates simulation results using the proposed timing diagram of Fig.3. The theoretical values of V_{op} and V_{om} are obtained from Eqs.(5) and (13). $D_i(i = 1, 2, 4, 5)$ is set to 0.25, 0.24, 0.25, and 0.24, so that we have $V_{op} = 8.0$V, $V_{om} = -5.15$V(Condition 3), and $D_i(i = 1, 2, 4, 5) = 0.25, 0.24, 0.20, 0.30$, $V_{op} = 8.0$V, $V_{om} = -8.0$V(Condition 4). We can see from Figs. 11(a) and 11(b) that V_{op} and V_{om} become theoretical values and V_{op} remains constant even with variations in V_{om}. The output voltage and its ripple voltage of these results are summarised in Tab.2. Simulation results

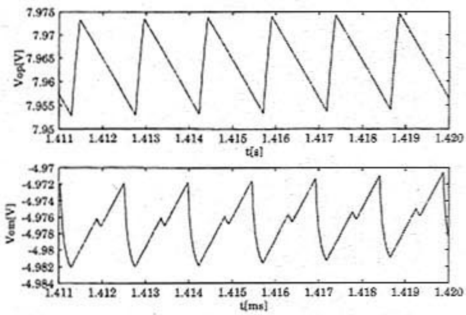

(a) Simulation results under condition 3. (V_{op}(upper) V_{om}(Bottom))

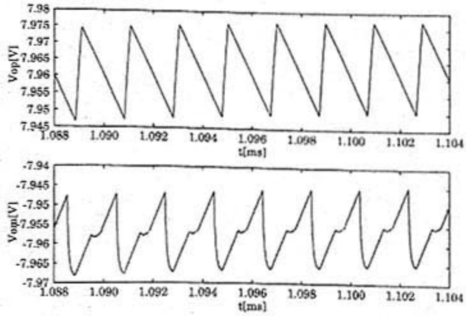

(b) Simulation results under condition 4. (V_{op}(upper) V_{om}(Bottom))

Fig. 11: Transient responses using the proposed timing diagram.

Table 2: Output voltage and its ripple voltage

	output voltage (positive)	ripple (positive)	output voltage (negative)	ripple (negative)
Condition 1 (Conventional)	6.9V	75.5mV	−5.9V	54.3mV
Condition 2 (Conventional)	8.2V	95.9mV	−7.2V	69.5mV
Condition 3 (Proposed)	7.97V	56.1mV	−4.98V	22.1mV
Condition 4 (Proposed)	7.97V	56.1mV	−7.97V	27.6mV

indicate that ripple voltage using the proposed timing diagram is less than that using the conventional one.

Figure 12 shows inductor current under condition 3. From the simulation results, the inductor

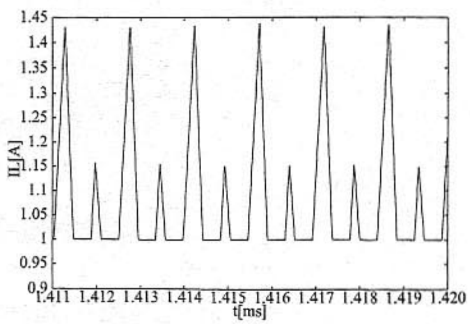

Fig. 12: Inductor current under conditions 3.

current ripple using the proposed timing diagram is obtained as 853.7mA.

Cross-regulation is a very important feature when SIMO is employed. Simulation results of output responses for output voltage variation are shown in Fig. 13. The output voltage is changed from steady-

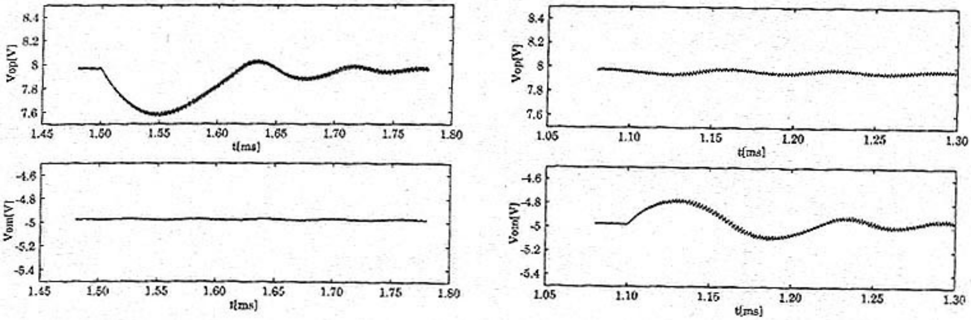

(a) positive output voltage. (b) negative output voltage.

Fig. 13: Output response for output voltage variation.

state value of each output voltage to 8V. Figures 13(a) and 13(b) exhibit cross-regulation characteristics for positive and negative output voltage, respectively. We can see from 13(b) that V_{om} does not change for the variation of V_{op} and cross-regulation is good performance thanks to PCCM.

Finally, Figure 14 shows power efficiency for the variation of load resistance from $R_o = 5\Omega$ to $R_o = 25\Omega$ in steps of 5Ω. The efficiency is defined as

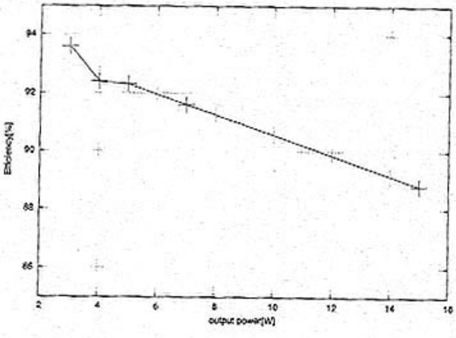

Fig. 14: efficiency of the proposed timing diagram

$$\frac{P_{po} + P_{no}}{P_i} \tag{14}$$

where P_{po}, P_{no}, P_i are positive output power, negative output power, and input power, respectively. From the simulation results, the efficiency using proposed timing diagram is as same as that using the conventional one.

Conclusion

A single inductor DC-DC converter with bipolar outputs using charge pump has been proposed. The conventional timing diagram used in the SIMO converter has a problem in that the negative output voltage depends upon the positive output voltage. The proposed timing diagram of bipolar outputs can be changed independently. Both a timing diagram and a control circuit are proposed. Spectre simulation results indicate that the negative output voltage using the proposed timing diagram can be controlled irrespective of the positive output variation while that using the conventional timing diagram depends on the positive output variation. Moreover, output voltage ripple and inductor current ripple using the proposed timing diagram are less than those in the conventional case. With the proposed timing diagram, the circuit can achieve goal cross-regulation performance.

References

[1] H.-P. Le, C.-S. Chae, K.-C. Lee, G.-H. Cho, S.-W. Wang, G.-H. Cho, and S. il Kim, "A single-inductor switching DC-DC converter with 5 outputs and ordered power-distributive control," in *Proc. of ISSCC,* no. 29.9, Feb. 2007, pp. 534-535.

[2] C.-S. Chae, H.-P. Le, K.-C. Lee, M.-C. Lee, G.-H. Cho, and G.-H. Cho, "A single-inductor step-up DC- DC switching converter with bipolar outputs for active matrix OLED mobile display panels," in *Proc. of ISSCC,* Feb. 2007, pp. 136-137.

[3] S.-C. Koon, Y.-H. Lam, and W.-H. Ki, "Integrated charge-control single-inductor dual-output step-up/step- down converter," in *Proc. of ISCAS,* May 2005, pp. 3071-3074.

[4] W.-H. Ki and D. Ma, "Single-inductor multiple-output switching converters," in *Proc. of Power Elec. Specialist Conf.*, June 2003.

[5] D. Ma, W.-H. Ki, C.-Y. Tsui, and P. K. T. Mok, "Single-inductor multiple-output switching converters with time-multiplexing control in discontinuous conduction mode," *IEEE Journal of Solid State Circuit,* vol. 38, no. 1, pp. 89-100, January 2003.

[6] W. Xu, X. Zhu, Z. Hong, and D. Killat, "Design of single-inductor dual-output switching converters with average current mode control," in *Proc. of APCCAS*, December 2008, pp. 902-905.

[7] S. A. Wibowo, I. Mori, K. Tsushida, S. Miwa, H. Kobayashi, T. Odaguchi, S. Takagi, S. Suzuki, I. Fukai, and J. Matsuda, "A Single-Inductor Dual-Output DC-DC Converter," *Proc. of The 22nd Workshop on Circuits and Systems in Karuizawa*, pp. 367-371, April 2009.

[8] Z. HU and D. MA, "A pseudo-CCM buck converter with freewheel switching control," in *Proc. of ISCAS,* May 2005, pp. 3083-3086.

[9] Y.-J. Woo, H.-P. Le, G.-H. Cho, G.-H. Cho, and S.-I. Kim, "Load-independent control of switching DC-DC converters with freewheeling current feedback," *IEEE Journal of Solid State Circuit*, vol. 43, no. 12, pp. 2798-2808, December 2008.

[10] D. Ma, W.-H. Ki, and C.-Y. Tsui, "A pseudo-ccm/dcm simo switching converter with freewheel switching," *IEEE Journal of Solid State Circuit*, vol. 38, no. 6, pp. 1007-1014, June 2003.

[11] N. Takai and Y. Fujimura, "Steep down-slope sawtooth wave generator utilizing two triangluar waves exclusively," *IEICE Transactions on Fundamentals*, vol. E92-A, no. 4, pp. 1019-1023, April 2009.